

1 A Simple Model of the Calvin Cycle Has Only One Physiologically Feasible Steady State  
2 under the Same External Conditions

3

4 Xin-Guang Zhu, Eric de Sturler, Rafael Alba, Stephen P. Long

5

6

7 Keywords: Nonlinear system; photosynthesis; steady state; evolution

8

9 **Abstract:** Most current photosynthesis research implicitly assumes that the  
10 photosynthetic process occurs only at one steady state. However, since the rate of each  
11 reaction in photosynthesis depends nonlinearly on its substrates and products, in theory,  
12 photosynthesis can have multiple steady states under given external conditions (i.e., in a  
13 given environment). The number of steady states of photosynthesis under the same  
14 external conditions has not been studied previously. Using the root finding program  
15 POLSYS\_PLP (Wise *et al* 2000, *ACM Transactions on Mathematical Software*), we  
16 study the number of potential steady states of a simplified model of the Calvin cycle. Our  
17 results show that the simplified model of the Calvin cycle can reside in multiple steady  
18 states, but that only one of these is physiologically feasible. We discuss the results from  
19 an evolutionary perspective.

20

This work was supported, in part, by the U.S. National Science Foundation under  
Grant IBN 04-17126.

## Introduction

1  
2  
3 Photosynthesis is inherently a complex system. It includes biophysical and biochemical  
4 reactions associated with light energy absorption, conversion of light energy into  
5 chemical energy in the form of ATP and NADPH, and complex biochemical reactions  
6 involved in the photosynthetic carbon metabolism. The rate of each reaction in  
7 photosynthesis depends nonlinearly on the concentrations of its substrates and products.  
8 Photosynthesis shows the typical characteristics of complex dynamical systems, such as  
9 oscillations, see, e.g., [1, 29, 30]. In fact, leaves show oscillations of CO<sub>2</sub> uptake, O<sub>2</sub>  
10 evolution, and chlorophyll fluorescence when either light or CO<sub>2</sub> varies, see e.g., [32].  
11 Another important characteristic of most dynamical systems is that they have multiple  
12 steady states [29, 30, 38]. For example, in a recent numerical study [38], Zwolak et al.  
13 showed that the cell cycle can exist in four different steady states if total cyclin is within  
14 a certain range. Even though photosynthesis is one of the most important plant  
15 physiological processes on earth, the number of potential steady states has not been well  
16 studied.

17  
18 Although it is extremely difficult to study the number of steady states for the complete  
19 photosynthetic process, some previous studies suggested that the CO<sub>2</sub> fixation process in  
20 photosynthesis, i.e., the Calvin cycle, might be able to exist in two different steady states  
21 [24, 25]. For example, Poolman et al. [25] showed that photosynthesis resided in two  
22 different steady states in leaves of different age when capacities to utilize the final  
23 carbohydrate product of photosynthesis were different. Pettersson and Ryde-Pettersson  
24 [24] suggested that the Calvin cycle showed two different steady states when the  
25 cytosolic phosphate concentration was below 1.9 mM. In contrast with this theoretical  
26 study [24], experiments only showed one steady state, e.g., [6, 10, 24]. These  
27 observations however lead to the important question, how many steady states  
28 photosynthesis can potentially reside in under the same external conditions. Currently, no  
29 experimental protocol is available to screen the number of potential steady states of  
30 photosynthesis. However, building mathematical models of photosynthesis and then  
31 identifying all steady-state solutions of the model appears a feasible route to tackle this

1 problem. Recently, robust numerical methods for solving polynomial systems of  
2 equations have become available. In particular, the globally convergent, probability-one  
3 homotopy method is guaranteed to find all isolated solutions to polynomial systems of  
4 equations; this method has been implemented in the numerical package POLSYS\_PLP  
5 [34]. The use of this package to analyze steady states of a biological problem is described  
6 in [5]. Following the approach in [5], we explore the number of steady states in a  
7 simplified model of the Calvin cycle derived from our photosynthesis model in [37].  
8 Specifically, we first rewrite the differential equations into a system of polynomial  
9 equations and set (equate) the right hand sides of the differential equations to zero. Next,  
10 we use the POLSYS\_PLP package to compute all isolated solutions of the polynomial  
11 system. Finally, we evaluate the physiological feasibility of the solutions found to  
12 identify biologically relevant steady states. Based on our results we discuss implications  
13 of the number of steady states from an evolutionary perspective and provide comparisons  
14 with previous studies [24, 25]. Under rare conditions it is possible that a dynamical  
15 system has steady-states that are not isolated (and hence POLSYS-PLP may not identify  
16 them); we assume this is not the case for the Calvin cycle and we will not consider this  
17 here.

18

## 19 **Method**

20 This section is divided into three subsections. First, we describe a simplified kinetic  
21 model of the Calvin cycle; second, we describe the procedure to find the steady state  
22 solutions of a dynamical system; and third, we describe the numerical experiments to  
23 identify all physiologically feasible solutions of the simplified model for the Calvin  
24 cycle.

25

### 26 **I. A simplified model of the Calvin cycle**

27 Our simplified model of the Calvin cycle has two sets of equations, namely, (a) rate  
28 equations and (b) differential equations.

#### 29 a) Rate equations

30 The reactions in the Calvin cycle are shown in Fig 1. Although the diagram represents a

1 simplified Calvin cycle, it includes the two major characteristics of the Calvin cycle: the  
2 autocatalytic cycle and photosynthate (including 3-Phosphoglycerate (PGA) and  
3 Glyceraldehyde 3-phosphate (GAP)) utilization. We assume that all reactions obey  
4 Michaelis-Menten kinetics. For a non-reversible reaction,  $A+B \rightarrow C + D$ , the generalized  
5 rate equation is:

6

$$7 \quad v = V_m \frac{A \times B}{(A + K_{mA})(B + K_{mB})} \dots\dots(1)$$

8 after [27], where  $K_{mA}$  and  $K_{mB}$  are the Michaelis-Menten constants of substrate A and B  
9 respectively, and  $A$  and  $B$  represent the concentrations of the respective substrates. The  
10 complete set of rate equations is summarized in Appendix A. We obtained the relevant  
11 constants/parameters by surveying the peer-reviewed literature (see Appendix B for  
12 sources). The Michaelis-Menten constants for the PGA and GAP utilization were  
13 estimated to ensure realistic rates of PGA and GAP utilization.

#### 14 b) Differential equations

15 The rate of change of each metabolite concentration is given by the difference between  
16 the rate(s) of the reaction(s) generating the metabolite and the rate(s) of the reaction(s)  
17 consuming the metabolite. For example, RuBP is generated from the phosphorylation of  
18 Ru5P ( $v_{13}$ ) via Ru5P kinase and consumed through RuBP carboxylation ( $v_1$ ) via Rubisco  
19 (Fig. 1). Thus, the rate of RuBP concentration change is

20

$$21 \quad \frac{d[\text{RuBP}]}{dt} = v_{13} - v_1 \dots\dots(2)$$

22

23 The differential equations describing the rate of change for each metabolite concentration  
24 form a system of coupled differential equations that represents a simplified model of the  
25 Calvin cycle (Appendix A). We use the routine *ode15s* from MATLAB® [19] to solve  
26 this system of differential equations, using the following initial concentrations: [RuBP]=2  
27 mM; [PGA]=2.4 mM; [DPGA] = 1mM; [GAP]=1 mM; and [Ru5P]=1 mM cf. [9]. After  
28 400 s (seconds), the system reaches a steady state. Subsequently, at 650 s, we perturb the  
29 system with a constant RuBP concentration for 50 seconds to check how the system

1 responds to a perturbation in an individual metabolite concentration. The photosynthetic  
 2 CO<sub>2</sub> uptake rate is calculated based on the rate of RuBP carboxylation. The  
 3 photosynthetic CO<sub>2</sub> uptake rate calculated from the model has a unit of mmol l<sup>-1</sup> s<sup>-1</sup> on  
 4 stroma volume basis (stroma is the space where the reactions in the Calvin cycle take  
 5 place). This calculated rate is converted into leaf area basis by assuming that 1 mmol l<sup>-1</sup> s<sup>-1</sup>  
 6 <sup>1</sup> corresponds to 33.3 μmol m<sup>-2</sup> s<sup>-1</sup> on leaf area basis [9]. Furthermore, we assume 1 gram  
 7 of chlorophyll in 1 m<sup>2</sup> leaf area and 30 ml stroma per gram chlorophyll [9].

8

## 9 **II. The procedure to find all isolated steady-state solutions**

10

11 The system of ordinary differential equations describing the simplified Calvin cycle can  
 12 be succinctly represented as:

$$13 \frac{dY}{dt} = f(Y, t, C), \dots\dots(3)$$

14 where  $Y$  is a vector of metabolite concentrations,  $t$  is time, and  $C$  represents parameters or  
 15 constants used in the model.

16

17 To obtain all steady-state solutions of this dynamical system (for a number of parameter  
 18 sets), we consider the system of nonlinear equations obtained from setting the right hand  
 19 side of (3) to zero. The solutions to this system of nonlinear equations are the steady state  
 20 solutions of (3). For example, the differential equation for RuBP can be transformed as  
 21 follows:

$$22 \frac{V_{13\max} \times \text{Ru5P} \times \text{ATP}}{(\text{Ru5P} + K_{m131}) \times (\text{ATP} + K_{m132})} - \frac{V_{1\max} \times \text{RuBP}}{\text{RuBP} + K_{m1}} = 0 \quad \dots\dots 4$$

23

24 Following the procedure of Zwolak et al [38], we transform all the differential equations  
 25 (Appendix A) into nonlinear polynomial equations, and then we use POLSYS\_PLP to  
 26 identify all the isolated roots. We develop a PERL script (RootFinder.pl) to generate the  
 27 required input for POLSYS\_PLP.

28

## 29 **III. Identifying all isolated solutions of the simplified model of the Calvin cycle.**

1 We compute all the (isolated) solutions of the simplified model of the Calvin cycle for  
2 the default values of all parameters (the maximal enzyme activities, i.e.,  $V_{max}$ , for each  
3 chemical reaction) and identify the physiologically feasible ones. In addition, we explore  
4 solutions of the model when the  $V_{max}$  of each enzyme (governing a chemical reaction)  
5 involved in the model is varied between 50% and 300% of the default (Appendix B).  
6 When varying the  $V_{max}$  of one enzyme (the  $V_{max}$  for a specific reaction), we kept activities  
7 of all other enzymes at their default values.

8

9

### Results

10 Fig 2 shows that the system of coupled differential equations quickly moves to a steady  
11 state (at about 400 s), where the steady-state concentration of each metabolite is within its  
12 physiologically relevant concentration range, cf. [9]. Moreover, the photosynthetic CO<sub>2</sub>  
13 uptake rate is also within the range of field-measured *rates* [36]. This suggests that the  
14 system of coupled differential equations (Appendix A) effectively simulates the CO<sub>2</sub>  
15 uptake rate. At 650 s, the system is perturbed from its steady state by enforcing a constant  
16 RuBP concentration for 50 seconds. This external perturbation effectively drives the  
17 concentrations of all metabolites in the system away from their steady-state  
18 concentrations. Upon removal of this perturbation, the system returns to its (original)  
19 physiologically feasible steady state in about 200 s, suggesting that our simple model is  
20 consistent with photosynthesis performance of actual plants in the lab, cf. [22]. For the  
21 default values of the model parameters (see Appendix B), POLSYS\_PLP finds 40  
22 solutions. A solution is considered to be physiologically feasible only if the concentration  
23 of each metabolite falls within its physiologically relevant range (0.0001 ~5 mM) [9].  
24 Out of 40 solutions, 39 solutions have concentrations with values that are too close to  
25 zero or negative or complex. Only one solution is physiologically feasible (see Appendix  
26 C for a sample solution). Under variation of the  $V_{max}$  (parameter) for each reaction the  
27 total number of solutions does not change; more importantly, the system still has only  
28 one solution that is physiologically feasible. This demonstrates the relevance of our study  
29 to a wide variety of plant species, which may have different enzyme concentrations and  
30 hence different maximal reaction rates. Table 1 shows the total number of solutions, the  
31 number of real solutions, the number of physiologically feasible real solutions, and the

1 number of physiologically non-feasible solutions when  $V_{max}$  of one enzyme is doubled  
2 (Table 1).

3  
4 The physiologically feasible solutions and solutions with values close to zero are shown  
5 in Fig 3 and 4. The substrate or product of the reaction for which  $V_{max}$  is modified (shown  
6 at top left corner) shows the greatest steady-state concentration change (Fig 3). For  
7 example, when  $V_{3max}$ , the maximal rate of the GAP dehydrogenase, is modified, the  
8 concentration of DPGA shows the greatest change in its steady-state concentration. For  
9 low GAP dehydrogenase activity, the DPGA concentration is higher than for high GAP  
10 dehydrogenase activity (Fig 3B), because with a higher enzyme activity a lower substrate  
11 concentration is needed to maintain the same flux rate through the reaction. On the other  
12 hand, metabolites that are ‘far’ from the reaction with modified enzyme activity show  
13 little or no change in concentration, where ‘far’ refers to the minimum number of  
14 reactions that link a metabolite to the reaction with modified activity. For example, when  
15  $V_{I_{max}}$ , the maximal activity of the enzyme Rubisco, is modified, the steady state  
16 concentration of Ru5P shows a negligible change (Fig 3A).

17  
18 We observe that the Calvin cycle has a physiologically feasible steady state for a wide  
19 range of maximal activities of Rubisco, GAP dehydrogenase, Phosphoribulose kinase,  
20 and the enzyme converting GAP to Ru5P (Fig. 3). However, when the maximal activities  
21 of either PGA kinase or PGA utilization are altered, the simplified model of the Calvin  
22 cycle loses its physiologically feasible solution and switches to a steady state where the  
23 concentrations of all metabolites are (too) close to zero (Fig. 4).

## 24 25 **Discussion**

26  
27 As photosynthesis, including both the light reactions and the carbon metabolism, is a  
28 complex dynamical system governed by coupled nonlinear differential equations, one  
29 might expect photosynthesis to have multiple steady states under the same light, CO<sub>2</sub> and  
30 O<sub>2</sub> conditions (the external conditions considered). So far, there has been no analysis to  
31 characterize the number of steady states of the entire photosynthesis system, partly due to

1 the lack of appropriate tools for such an analysis. As the first step, this study uses the  
2 package POLSYS\_PLP to identify steady-state solutions corresponding to isolated  
3 solutions of the associated polynomial system of equations representing a simplified  
4 model of the Calvin cycle. It is surprising that even though 40 solutions are identified for  
5 the simplified Calvin cycle, only one of them is physiologically feasible.

6  
7 Although the model of the Calvin cycle we use in this study is relatively simple, it  
8 possesses the two key characteristics of the Calvin cycle: (1) the autocatalytic cycle and  
9 (2) the utilization of photosynthate (i.e., GAP and PGA) (Fig 1). It is intriguing that only  
10 one physiologically feasible steady state is found under the given external conditions  
11 ( $\text{CO}_2$ ,  $\text{O}_2$ , light intensity). Studies in the past have suggested multiple steady states. In  
12 [25] Poolman et al. demonstrated that the Calvin cycle can potentially exist in different  
13 steady states for leaves at different ages and at different external conditions. However,  
14 whether photosynthesis can reside in two different states for the same leaf age under the  
15 same external conditions was not studied [25]. Pettersson and Ryde-Pettersson [24]  
16 showed that the Calvin cycle had two feasible steady states, one with high flux rate and  
17 another with low flux rate. The Calvin cycle model used in this study is simpler than that  
18 of Pettersson and Ryde-Pettersson [24], which might explain the differences in the  
19 number of steady states identified. On the other hand, all previous experiments on real  
20 plants showed that photosynthesis only exists in one steady state under a fixed set of  
21 external conditions [16, 31], while dramatic changes in the external conditions (for  
22 example, from very low light to very high light) may lead to long transient phases marked  
23 by significant oscillations [8, 32]. The accuracy of the Farquhar et al [4] model to predict  
24 the photosynthetic  $\text{CO}_2$  uptake rate under a wide variety of external conditions also  
25 suggests that photosynthesis exists only in one steady state under fixed conditions. Given  
26 these partially contradictory results, a detailed analysis of the number of potential steady  
27 states for a complete model of the photosynthetic carbon metabolism [37] will be  
28 required to ultimately determine whether photosynthesis has the potential to exist in  
29 multiple steady states in a leaf and if so what mechanisms prevent it from switching  
30 freely between different steady states.

31

1 Existing experimental evidence suggests that in the field photosynthesis stays  
2 predominantly if not always in one steady state under given external conditions [4, 10,  
3 24]. If this is true, then what is the advantage of staying in only one steady state? If  
4 photosynthesis has multiple steady states with each having different photosynthetic CO<sub>2</sub>  
5 uptake rate, it would be advantageous for photosynthetic cells to stay in the steady state  
6 with a higher photosynthetic CO<sub>2</sub> uptake rate. It is possible that during evolution  
7 mechanisms evolved to keep photosynthesis operating only in the state with high  
8 photosynthetic CO<sub>2</sub> uptake rate. In line with this idea, the structure of the Calvin cycle  
9 has been conserved from cyanobacteria all the way through high plants [20, 33], possibly  
10 for the purpose of staying in the steady state with the higher photosynthetic CO<sub>2</sub> uptake  
11 rate. It is possible that various mechanisms of enzyme activity regulation, e.g.,  
12 modification of the redox state of Ferredoxin-Thioredoxin system, or pH of stroma, or  
13 Mg<sup>2+</sup> concentration [18, 26] might be involved in keeping photosynthesis operating in a  
14 state with high photosynthetic CO<sub>2</sub> uptake rate.

15

16 In summary, this theoretical study explored a number of potential steady states of a  
17 simplified model of the Calvin cycle. Results from this and previous studies suggest that,  
18 although the Calvin cycle has the potential to stay in multiple steady states, it seems to  
19 stay only in one steady state. This property of the Calvin cycle might be a result of the  
20 natural selection for a higher CO<sub>2</sub> uptake rate. A detailed study of the number of steady  
21 states for a complete model of photosynthesis is needed to identify the total potential  
22 number of steady states of photosynthesis in the field.

23

24

#### ACKNOWLEDGEMENTS

25

26 This research was supported by the National Center for Supercomputing Applications,  
27 the National Science Foundation, IBN 04-17126, and the McNair Scholars Program of  
28 the University of Illinois.

## 1 REFERENCES

- 2 [1] R. Albert, H. Jeong, A.L. Barabasi, Error and attack tolerance of complex  
3 networks, *Nature* 406 (2000) 378-382.
- 4 [2] J.A. Bassham, G.H. Krause, Free energy changes and metabolic regulation in  
5 steady state photosynthetic carbon reduction, *Biochim. Biophys. Acta* 189 (1969)  
6 207-221.
- 7 [3] R. Cerf, Glyceraldehyde 3-phosphate dehydrogenase (NADP) from *Sinapis alba*:  
8 steady state kinetics, *Phytochemistry* 17 (1978) 2061-2067.
- 9 [4] G.D. Farquhar, S. von Caemmerer, J.A. Berry, A biochemical model of  
10 photosynthetic CO<sub>2</sub> assimilation in leaves of C<sub>3</sub> species, *Planta* 149 (1980) 78-90.
- 11 [5] G. Ferri, G. Comerio, P. Iadarola, M.C. Zapponi, M.L. Speranza, Subunit  
12 structure and activity of glyceraldehyde-3-phosphate dehydrogenase from spinach  
13 chloroplasts, *Biochim. Biophys. Acta* 522 (1978) 19-31.
- 14 [6] U.-I. Flugge, M. Freisl, H.W. Heldt, Balance between metabolite accumulation  
15 and transport in relation to photosynthesis by isolated spinach chloroplasts, *Plant*  
16 *Physiol.* 65 (1980) 574-577.
- 17 [7] A. Gardemann, M. Stitt, H.W. Heldt, Control of CO<sub>2</sub> fixation - regulation of  
18 spinach ribulose-5-phosphate kinase by stromal metabolite levels, *Biochim.*  
19 *Biophys. Acta* 722 (1983) 51-60.
- 20 [8] K.R. Hanson, Steady-state and oscillating photosynthesis by a starchless mutant  
21 of *Nicotiana glauca*, *Plant Physiol.* 93 (1990) 1212-1218.
- 22 [9] G.C. Harris, M. Koniger, The 'high' concentration of enzymes within the  
23 chloroplast, *Photosyn. Res.* 54 (1997) 5-23.
- 24 [10] H.W. Heldt, C.J. Chon, D. Maronde, A. Herold, Z.S. Stankovic, D.A. Walker, A.  
25 Kraminer, M.R. Kirk, U. Heber, Role of orthophosphate and other factors in  
26 regulation of starch formation in leaves and isolated chloroplasts, *Plant Physiol.*  
27 59 (1977) 1146-1155.
- 28 [11] A.U. Igamberdiev, N.V. Bykova, P.J. Lea, P. Gardestrom, The role of  
29 photorespiration in redox and energy balance of photosynthetic plant cells: a  
30 study with a barley mutant deficient in glycine decarboxylase, *Physiol. Plant.* 111  
31 (2001) 427-438.
- 32 [12] E. Kopkesecondo, I. Molnar, C. Schnarrenberger, Isolation and characterization  
33 of the cytosolic and chloroplastic 3-phosphoglycerate kinase from spinach leaves,  
34 *Plant Physiol.* 93 (1990) 40-47.
- 35 [13] W.A. Laing, M. Stitt, H.W. Heldt, Control of CO<sub>2</sub> fixation - changes in the  
36 activity of ribulosephosphate kinase and fructose-bisphosphatase and  
37 sedoheptulose-bisphosphatase in chloroplasts, *Biochim. Biophys. Acta* 637 (1981)  
38 348-359.
- 39 [14] M. Larsson-Raznikiewicz, Kinetic studies on the reaction catalyzed by  
40 phosphoglycerate kinase. II. The kinetic relationships between 3-  
41 phosphoglycerate, MgATP<sup>2-</sup> and activating metal ion, *Biochim. Biophys. Acta*  
42 132 (1967) 33-40.
- 43 [15] E. Latzko, M. Steup, C. Schachtele, Starch synthesis and degradation in  
44 photosynthetic tissues, In: G. Akoyunoglou (Eds.), *Photosynthesis, IV Regulation*  
45 *of Carbon Metabolism*. Balaban International Science Services, Philadelphia,  
46 1981, pp. 517-528.

- 1 [16] S.P. Long, P.K. Farage, R.L. Garcia, Measurement of leaf and canopy  
2 photosynthetic CO<sub>2</sub> exchange in the field, *J. Exp. Bot.* 47 (1996) 1629-1642.
- 3 [17] J. Macioszek, L.E. Anderson, Changing kinetic properties of the 2-enzyme  
4 phosphoglycerate kinase NADP-linked glyceraldehyde-3-phosphate  
5 dehydrogenase couple from pea chloroplasts during photosynthetic induction,  
6 *Biochim. Biophys. Acta* 892 (1987) 185-190.
- 7 [18] W. Martin, R. Scheibe, C. Schnarrenberger, The Calvin cycle and its regulation,  
8 In: R. C. Leegood, T. D. Sharkey, S. von Caemmerer (Eds.), *Advances in*  
9 *Photosynthesis Vol 9*, Kluwer Academic Publishers, Dordrecht, 2000, pp. 9-51.
- 10 [19] MATLAB, version 6. Mathworks inc., Matick, MA, USA, 2006.
- 11 [20] A.Y. Mulkidjanian, E.V. Koonin, K.S. Makarova, S.L. Mekhedov, A. Sorokin,  
12 Y.I. Wolf, A. Dufresne, F. Partensky, H. Burd, D. Kaznadzey, R. Haselkorn,  
13 M.Y. Galperin, The cyanobacterial genome core and the origin of photosynthesis,  
14 *PNAS* 103 (2006) 13126-13131.
- 15 [21] J. Omnaas, M.A. Porter, F.C. Hartman, Evidence for a reactive cysteine at the  
16 nucleotide binding-site of spinach ribulose-5-phosphate kinase, *Arch. Biochem.*  
17 *Biophys.* 236 (1985) 646-653.
- 18 [22] R.W. Percy, L.J. Gross, D. He, An improved dynamic model of photosynthesis  
19 for estimation of carbon gain in sunfleck light regimes, *Plant, Cell Environ.* 20  
20 (1997) 411-424.
- 21 [23] A. Peterkofsky, E. Racher, The reductive pentose phosphate cycle III, enzyme  
22 activities in cell-free extracts of photosynthetic organisms, *Plant Physiol.* 36  
23 (1961) 409-414.
- 24 [24] G. Pettersson, U. Ryde-Pettersson, A mathematical model of the Calvin  
25 photosynthesis cycle, *Eur. J. Biochem.* 175 (1988) 661-672.
- 26 [25] M.G. Poolman, H. Olcer, J.C. Lloyd, C.A. Raines, D.A. Fell, Computer modelling  
27 and experimental evidence for two steady states in the photosynthetic Calvin  
28 cycle, *Eur. J. Biochem.* 268 (2001) 2810-2816.
- 29 [26] P. Schurmann, J.P. Jacquot, Plant thioredoxin systems revisited, *Ann. Rev. Plant*  
30 *Physiol. Plant Mol. Biol.* 51 (2000) 371-400.
- 31 [27] I.H. Segel, *Enzyme Kinetics*, John Wiley & Sons Inc., New York, 1975.
- 32 [28] P. Trost, S. Scagliarini, V. Valenti, P. Pupillo, Activation of spinach chloroplast  
33 glyceraldehyde-3-phosphate dehydrogenase - effect of glycerate 1,3-bisphosphate,  
34 *Planta* 190 (1993) 320-326.
- 35 [29] J.J. Tyson, K. Chen, B. Novak, Network dynamics and cell physiology, *Nature*  
36 *Rev. Mol. Cell Biol.* 2 (2001) 908-916.
- 37 [30] J.J. Tyson, K.C. Chen, B. Novak, Sniffers, buzzers, toggles and blinkers:  
38 dynamics of regulatory and signaling pathways in the cell, *Curr. Opin. Cell Biol.*  
39 15 (2003) 221-231.
- 40 [31] S. von Caemmerer, Biochemical models of leaf photosynthesis, In: *Techniques in*  
41 *Plant Sciences series*. CSIRO Publishing, Australia, 2000.
- 42 [32] D. Walker, Concerning oscillations, *Photosyn. Res.* 34 (1992) 387-395.
- 43 [33] Z. Wang, X.G. Zhu, Y.Z. Chen, Y.Y. Li, J. Hou, Y.X. Li, L. Liu, Exploring  
44 photosynthesis evolution by comparative analysis of metabolic networks between  
45 chloroplasts and photosynthetic bacteria, *BMC Genomics* 7 (2006). doi:  
46 10.1186/1471-2164-7-100

- 1 [34] S.M. Wise, A.J. Sommese, L.T. Watson, Algorithm 801: POLSYS\_PLP: a  
2 partitioned linear product homotopy code for solving polynomial systems of  
3 equations, ACM Trans. Math. Software 26 (2000) 176-2000.
- 4 [35] I.E. Woodrow, K.A. Mott, Modeling C<sub>3</sub> photosynthesis - a sensitivity analysis of  
5 the photosynthetic carbon reduction cycle, Planta 191 (1993) 421-432.
- 6 [36] S.D. Wullschleger, Biochemical limitations to carbon assimilation in C<sub>3</sub> plants - a  
7 retrospective analysis of the A/C<sub>i</sub> curves from 109 species, J. Exp. Bot. 44 (1993)  
8 907-920.
- 9 [37] X.-G. Zhu, E. de Sturler, S.P. Long, Optimizing the distribution of resources  
10 between enzymes of carbon metabolism can dramatically increase photosynthetic  
11 rate: A numerical simulation using an evolutionary algorithm, Plant Physiol. 145  
12 (2007) 513-526.
- 13 [38] J.W. Zwolak, J.J. Tyson, L.T. Watson, Finding all steady state solutions of  
14 chemical kinetic models, Nonlinear Anal. Real World Appl. 5 (2004) 801-814.  
15  
16

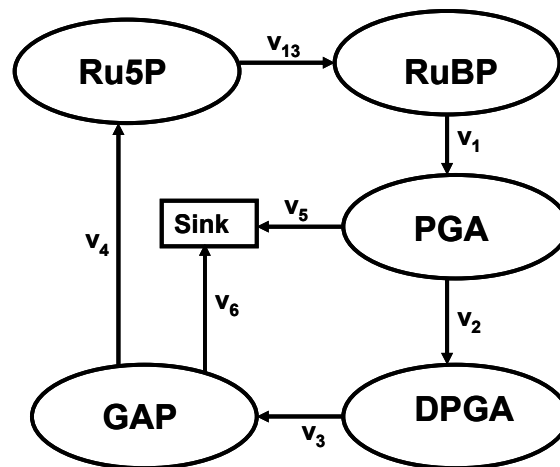
1 Table 1 The number of different types of roots when doubling maximal activities of  
 2 enzymes in the simplified model of the Calvin cycle. When doubling the maximal  
 3 activity of one enzyme, the maximal activities of other enzymes are assumed to be at  
 4 their default values. The concentration of ATP is assumed to be 0.5 mM [2, 11, 35]. The  
 5 column *Total* indicates the total number of solutions; the column *Real solutions* indicates  
 6 the number of real solutions. The real solutions were further differentiated as either  
 7 *physiologically feasible solutions* or *physiologically nonfeasible real solutions*.

8

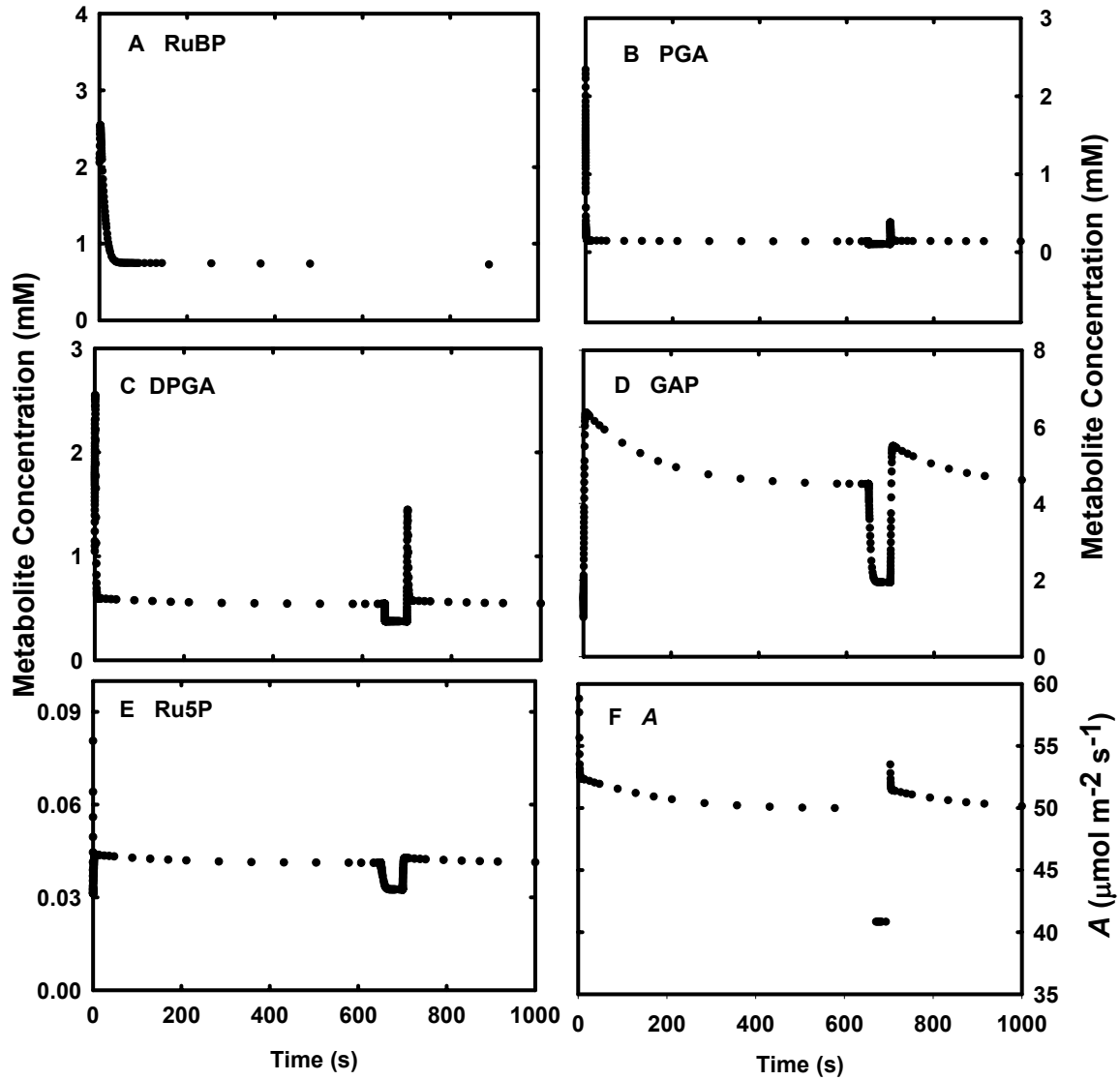
<u>Category</u>	<i>Total</i>	<i>Real solutions</i>	<i>Physiologically feasible real solutions</i>	<i>Physiologically nonfeasible real solutions</i>
<u><math>V_{\max}</math></u>				
$V_{1\max}$	40	5	1	4
$V_{2\max}$	40	4	0	4
$V_{3\max}$	40	4	1	3
$V_{4\max}$	40	5	1	4
$V_{5\max}$	40	4	0	4
$V_{13\max}$	40	5	1	4

9

- 1 Figure 1. The diagram showing reactions in the simplified model of the Calvin cycle.
- 2 RuBP: Ribulose 1,5-bisphosphate; PGA: 3-Phosphoglycerate; DPGA: 1,3-
- 3 Bisphoglycerate; GAP: Glyceraldehyde 3-phosphate; Ru5P: Ribulose 5-phosphate. The
- 4 symbol such as  $v_1, \dots, v_{13}$  represents the rate of each reaction in the diagram. Arrow
- 5 indicates the direction of a reaction. Sink represents utilization of PGA and GAP through
- 6 sucrose synthesis or starch synthesis.

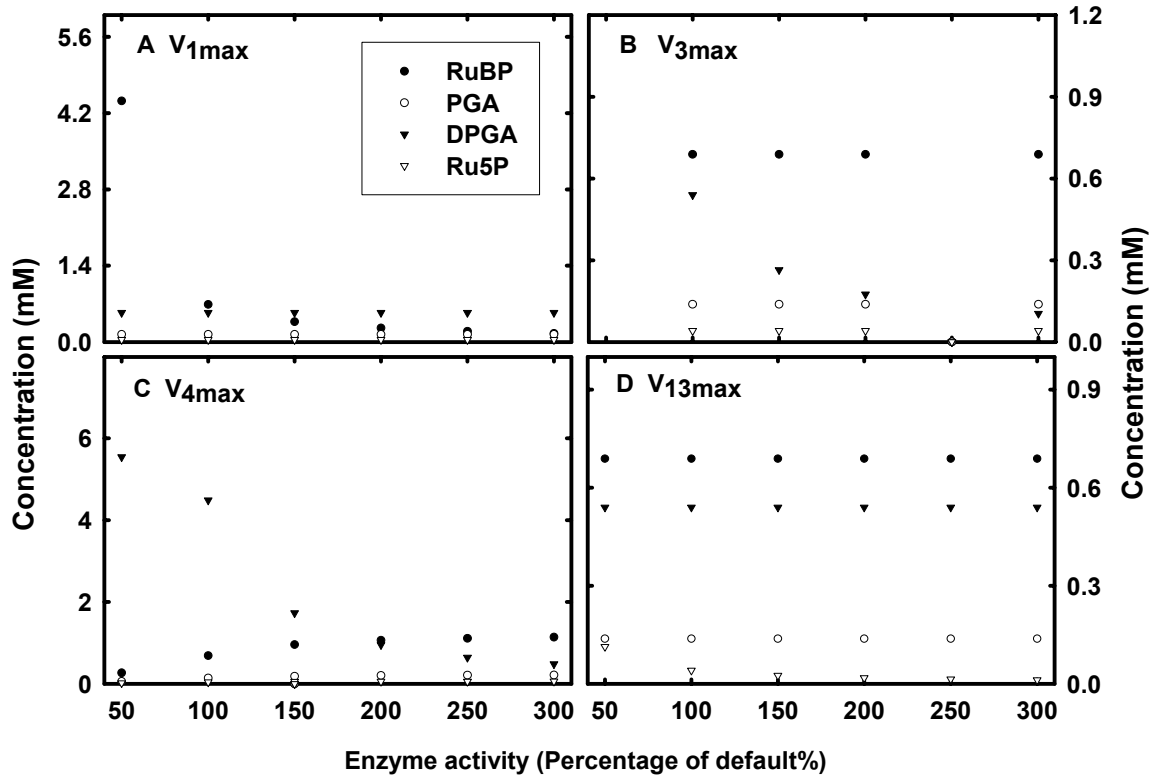


1 Fig 2. The simulated time evolution of different metabolite concentrations in the  
 2 simplified model of the Calvin cycle. The system (Appendix A) is perturbed at the 650  
 3 second by keeping the RuBP concentration at a constant 0.5 mM. At the 700 second, the  
 4 perturbation is removed. The system quickly moves to (and stabilizes at) its previous  
 5 steady state. *A*: photosynthetic CO<sub>2</sub> uptake rate.



6

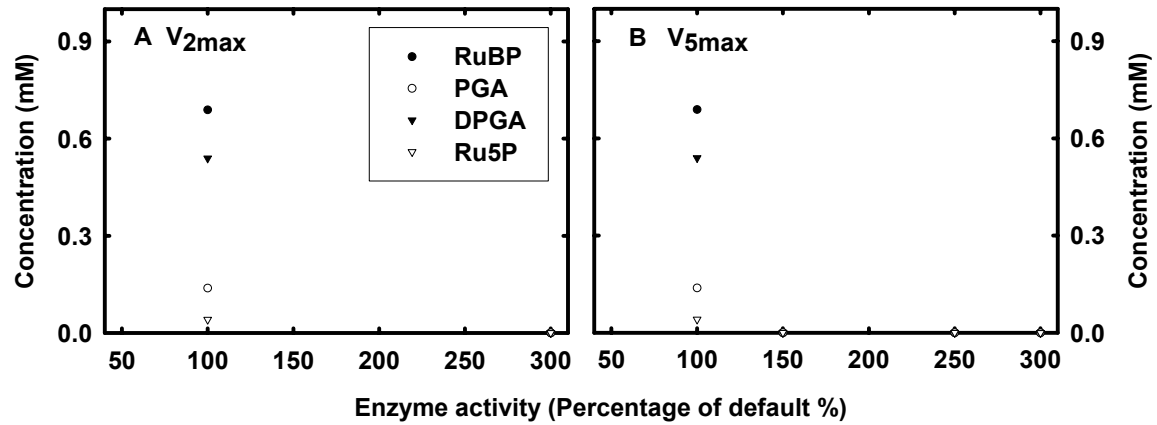
1 Figure 3 The physiologically feasible and the close-to-zero steady-state concentrations of  
 2 four metabolites in the simplified model of the Calvin cycle under different maximal  
 3 enzyme activities. In each panel, the maximal enzyme activity of one enzyme varies from  
 4 50% to 300% of its default value while the maximal enzyme activities of all other  
 5 enzymes are set to be at their default values. This figure shows that there is only one  
 6 physiologically feasible steady-state solution under the same external conditions.



7  
8

1

2 Fig 4. The physiologically feasible and the close-to-zero steady-state metabolite  
3 concentrations in the simplified Calvin cycle under different  $V_{2max}$  and  $V_{5max}$  (see  
4 Fig 3 for detailed legend).



5

1 Appendix A Equations used in the simplified model of the Calvin cycle

2

3 The differential equations:

$$\frac{d\text{RuBP}}{dt} = v_{13} - v_1$$

$$\frac{d\text{PGA}}{dt} = 2 \times v_1 - v_2 - v_5$$

4 
$$\frac{d\text{DPGA}}{dt} = v_2 - v_3$$

$$\frac{d\text{GAP}}{dt} = v_3 - v_4 - v_6$$

$$\frac{d\text{Ru5P}}{dt} = 0.6 \times v_4 - v_{13}$$

5

6 The rate equations:

$$v_1 = \frac{V_{1\max} \times \text{RuBP}}{(\text{RuBP} + K_{m1})}$$

7 
$$v_2 = \frac{V_{2\max} \times \text{PGA} \times \text{ATP}}{(\text{PGA} + K_{m21}) \times (\text{ATP} + K_{m22})}$$

$$v_3 = \frac{V_{3\max} \times \text{DPGA}}{\text{DPGA} + K_{m3}}$$

$$v_4 = \frac{V_{4\max} \times \text{GAP}}{\text{GAP} + K_{m4}}$$

8 
$$v_5 = \frac{V_{5\max} \times \text{PGA} \times \text{ATP}}{(\text{PGA} + K_{m51}) \times (\text{ATP} + K_{m52})}$$

$$v_6 = \frac{V_{6\max} \times \text{GAP}}{\text{GAP} + K_{m6}}$$

$$v_{13} = \frac{V_{13\max} \times \text{Ru5P} \times \text{ATP}}{(\text{Ru5P} + K_{m131}) \times (\text{ATP} + K_{m132})}$$

9

1 Appendix B Parameters used in the simplified model of the Calvin cycle

2

3 Table B1 The maximal activities ( $V_m$ ) of each enzyme in the simplified model of the  
4 Calvin cycle

5

Maximal Activity	Enzyme name	Reaction	$^aV_m$ mmol l <sup>-1</sup> s <sup>-1</sup>	Reference
V <sub>1</sub>	Rubisco	RuBP+CO <sub>2</sub> →2PGA	3.78	[15, 23, 35]
V <sub>2</sub>	PGA Kinase	PGA+ATP → ADP + DPGA	11.75	[15, 23, 35]
V <sub>3</sub>	GAP dehydragenase	DPGA+NADPH →GAP + OP+NADP	5.04	[15, 23, 35]
V <sub>4</sub>	Conversion of GAP into Ru5P	GAP→0.6Ru5P	3.05	Model estimate
V <sub>13</sub>	Ribulose biphosphate kinase	Ru5P+ATP→RuBP+ADP	8	[15, 23, 35]
V <sub>5</sub>	Sink capacity	PGA→ Sink	3	[15, 23, 35]
V <sub>6</sub>	Sink capacity	GAP→ Sink	0.1	Model estimate

6

1 Table B2 The Michaelis-Menten constants of enzymes used in the simplified model of  
 2 the Calvin cycle

3

RN <sup>a</sup>	Reaction	Parameter <sup>b</sup>	Value (mM)	Description <sup>c</sup>	Reference
1	RuBP+CO <sub>2</sub> →2PGA	K <sub>m13</sub>	1	RuBP	Model estimate, cf. [31]
2	PGA+ATP →ADP + DPGA	K <sub>m21</sub>	0.240	PGA	[12, 14]
2	PGA+ATP →ADP + DPGA	K <sub>m22</sub>	0.390	ATP	[12, 14]
3	DPGA+NADPH →GAP + OP+NADP	K <sub>m3</sub>	0.5	DPGA	Model estimate, cf. [3, 5, 17, 28]
4	GAP→ 0.6Ru5P	K <sub>m4</sub>	0.84	GAP	Model estimate
5	PGA→ Sink	K <sub>m5</sub>	0.75	PGA	Model estimate
6	GAP → Sink	K <sub>m6</sub>	5	GAP	Model estimate
13	Ru5P+ATP→RuBP+ADP	K <sub>m131</sub>	0.15	Ru5P	[7, 21]
13	Ru5P+ATP→RuBP+ADP	K <sub>m132</sub>	0.059	ATP	[7, 13, 21]

4

5 <sup>a</sup> RN: Reaction number corresponding to the number in Fig. 1.

6 <sup>b</sup> Parameters beginning  $K_M$  represent the apparent Michaelis-Menten constant of the  
 7 metabolite listed in the *description* column

8 <sup>c</sup> The description column lists the compounds to which the kinetic constant applies.

9

10

1 **Appendix C** Sample real solutions of the simplified model of the Calvin cycle  
2 Given a set of  $V_{\max}$  values, the system of nonlinear polynomials derived from the  
3 differential equations representing the simplified model of the Calvin cycle has 40 roots.  
4 Among them 4 – 5 were real definite roots. A set of sample real solutions for the model is  
5 shown below. In this sample, the  $V_{1\max}$  is set to be 200% of the default  $V_{1\max}$  and the  $V_{\max}$   
6 values of all other enzymes are set to be at their default values. X(1): RuBP, X(2) : PGA,  
7 X(3) : DPGA, X(4) : GAP, X(5): Ru5P. We can see that only the first real solution is a  
8 physiologically feasible solution.

9

10 Real solution 1

11 X(1)= 2.56097627171181E-01

12 X(2)= 1.38098652799639E-01

13 X(3)= 5.39698924750138E-01

14 X(4)= 4.48565670978998E+00

15 X(5)= 4.11198559296765E-02

16

17 Real solution 2

18 X(1)= -3.57848262985460E-17

19 X(2)= 8.75644031437841E-18

20 X(3) = 2.61129825157095E-18

21 X(4)= 1.75408016482927E-16

22 X(5)= 7.04135520029619E-18

23

24 Real solution 3

25 X(1)= 4.09031898442628E-01

26 X(2)= -5.50930499218444E-01

27 X(3)= -8.29333703387913E-01

28 X(4)= -5.05596520084859E+00

29 X(5)= 6.62434472205359E-02

30

31 Real solution 4

1 X(1)= -1.00000000089146E+00  
2 X(2)= -2.40000000104034E-01  
3 X(3)= -5.00000000152509E-01  
4 X(4)= -8.40000000156337E-01  
5 X(5)= -1.50000000126720E-01  
6  
7 Real solution 5  
8 X(1) = 5.55406405928947E-01  
9 X(2)= 3.80006541425408E-01  
10 X(3)= 3.37815725345562E+00  
11 X(4)= -2.60784352798313E+00  
12 X(5)= 9.06998056463301E-02